Supporting Information for

Microfluidics-based Single-Cell Protrusion Analysis for Rapid Screening Drugs Targeting Subcellular Mitochondrial Trafficking in Cancer Progression

Pengchao Zhang[1, 2], Jun Yao[3], Bin Wang[4], and Lidong Qin[1, 2, *]

[1]Department of Nanomedicine, Houston Methodist Research Institute, 6670 Bertner Ave, Houston, TX 77030, USA.

[2]Department of Cell and Developmental Biology, Weill Medical College of Cornell University, New York, NY 10065, USA.

[3]Department of Genetics and [4]Department of Molecular and Cellular Oncology, The University of Texas MD Anderson Cancer Center, Houston, TX 77030, USA.

This Supporting Information includes:

Figures S1-S8

Table S1

Movie S1-S4

Figures S1-S8

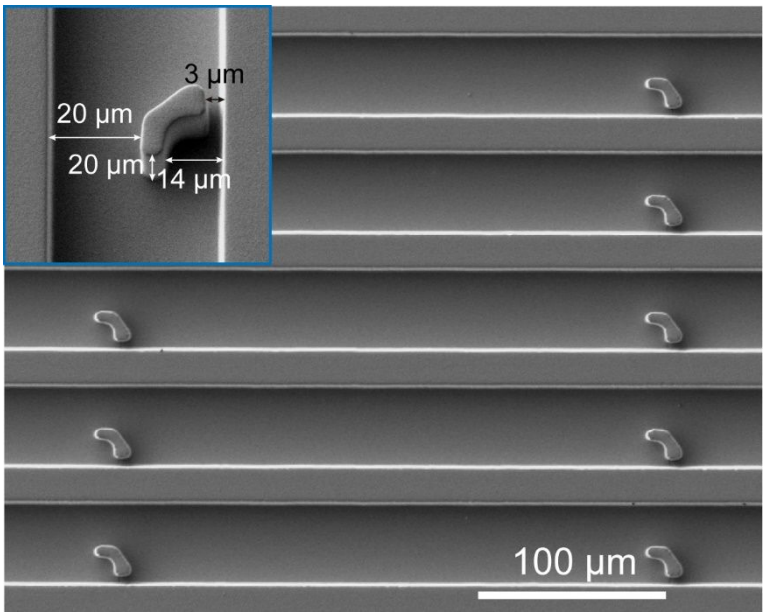

Figure S1. The morphology and parameters of the micro-hook arrays developed in this study.

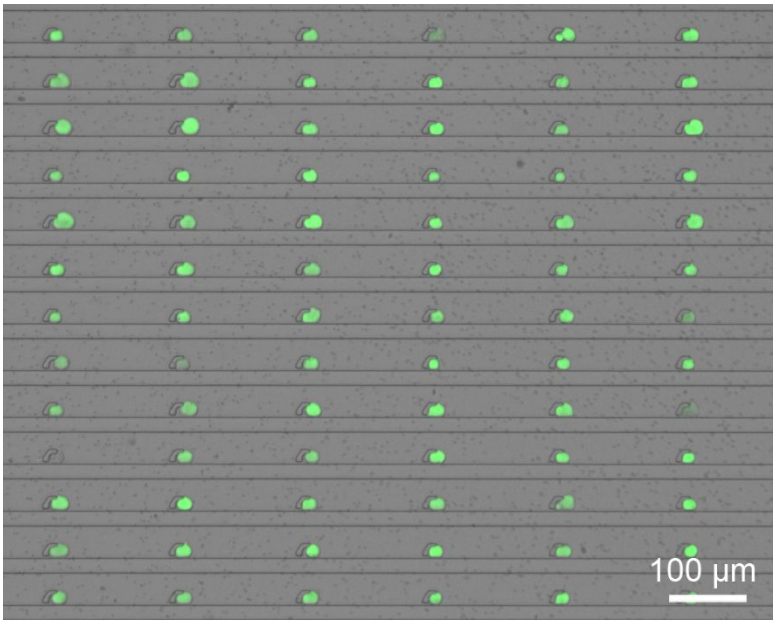

Figure S2. A representative image of the generated single cell array of MDA-MB-231/GFP using the PG-Chip.

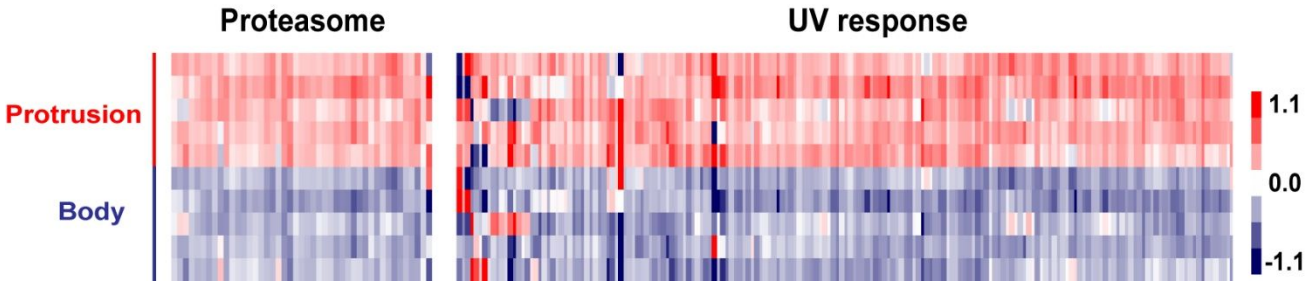

Figure S3. Heatmap the comparison of proteasome and UV response-related gene expression between cell protrusions and cell bodies.

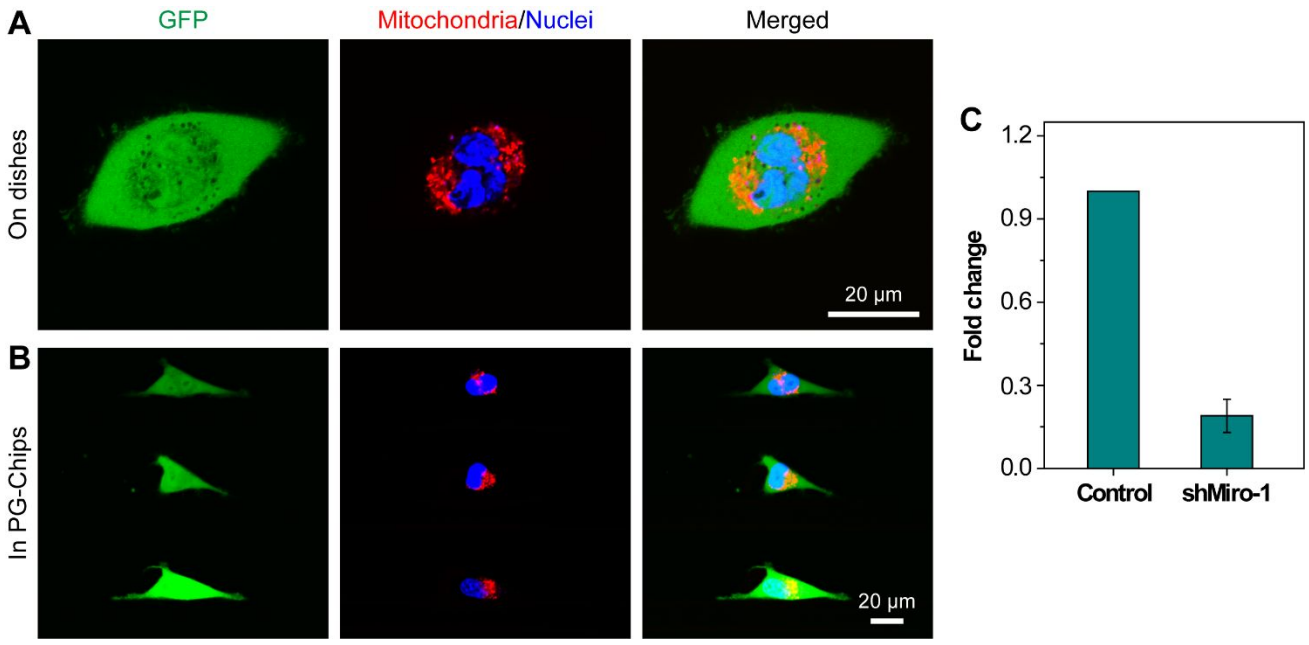

Figure S4. shRNA-mediated knockdown of Miro-1 inhibits subcellular mitochondrial trafficking. (A) Knockdown of Miro-1 in MDA-MB-231 cells induced the perinuclear localization of mitochondria affecting the fragmented morphology of mitochondria. (B) Miro-1 knockdown MDA-MB-231 cells shows shortened cell protrusions. Mitochondria and nuclei were labeled with MitoTracker Red and Hoechst 33342, respectively. (C) Validation of the knockdown of Miro-1 by qPCR analysis. β-actin (ACTB) was used as an endogenous control to normalize each sample. The expression level of Miro-1 was first nomalized to its corresoinding expression level of ACTB. Then the fold change was calculated by dividing the normalized expression level of Miro-1 in the knockdown cells by the normalized expression level of Miro-1 in the control cells. Data are expressed as mean ± S.D.

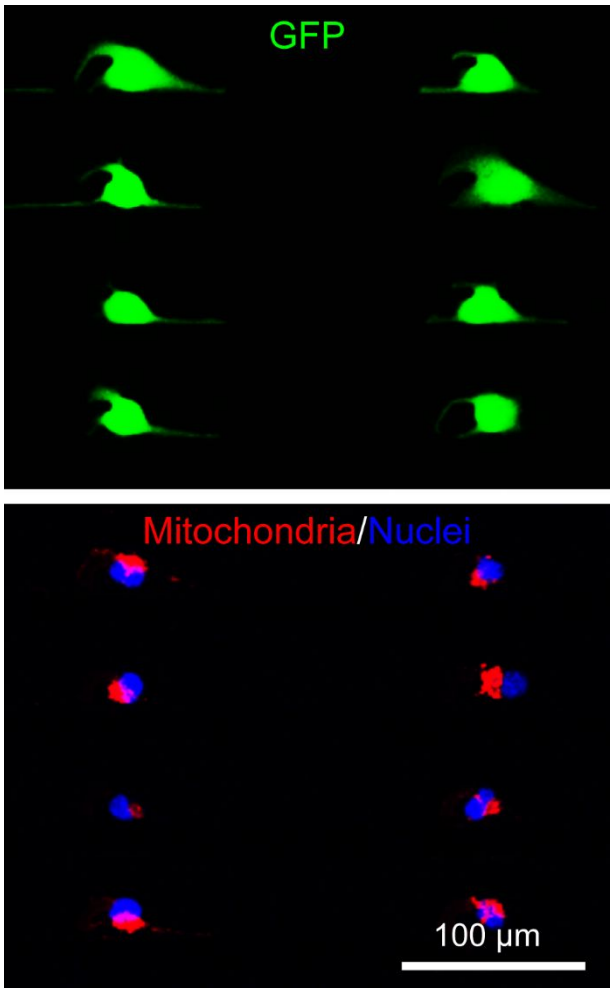

Figure S5. The perinuclear localization of mitochondria in chloroquine-treated (50 μM) MDA-MB-231/GFP cells in microfluidic chips. Mitochondria and nuclei were labeled with MitoTracker Red and Hoechst 33342, respectively.

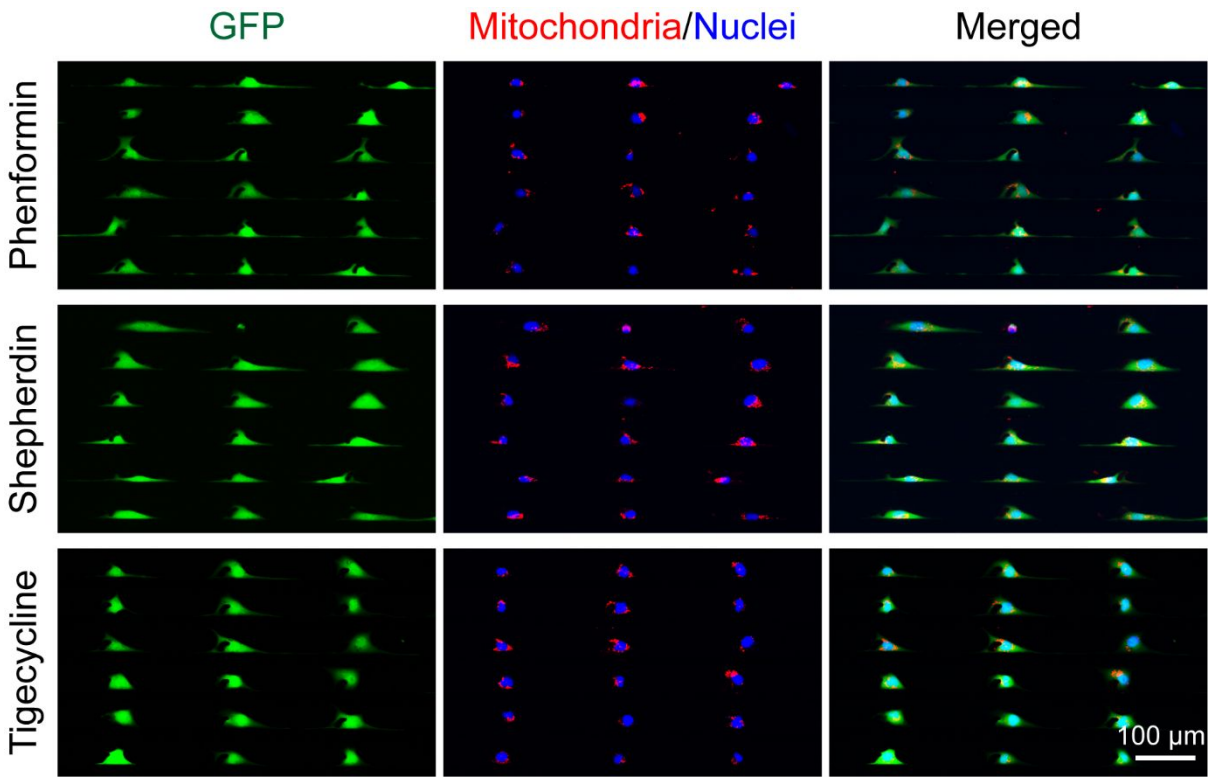

Figure S6. Morphology of MDA-MB-231/GFP cells treated with mitochondrial inhibitors and cultured in microfluidic chips for 6 h. After treatment, the cells displayed much shorter cell protrusions. Mitochondrial staining showed perinuclear localization rather than trafficking to the protrusions. Mitochondria and nuclei were labeled with MitoTracker Red and Hoechst 33342, respectively.

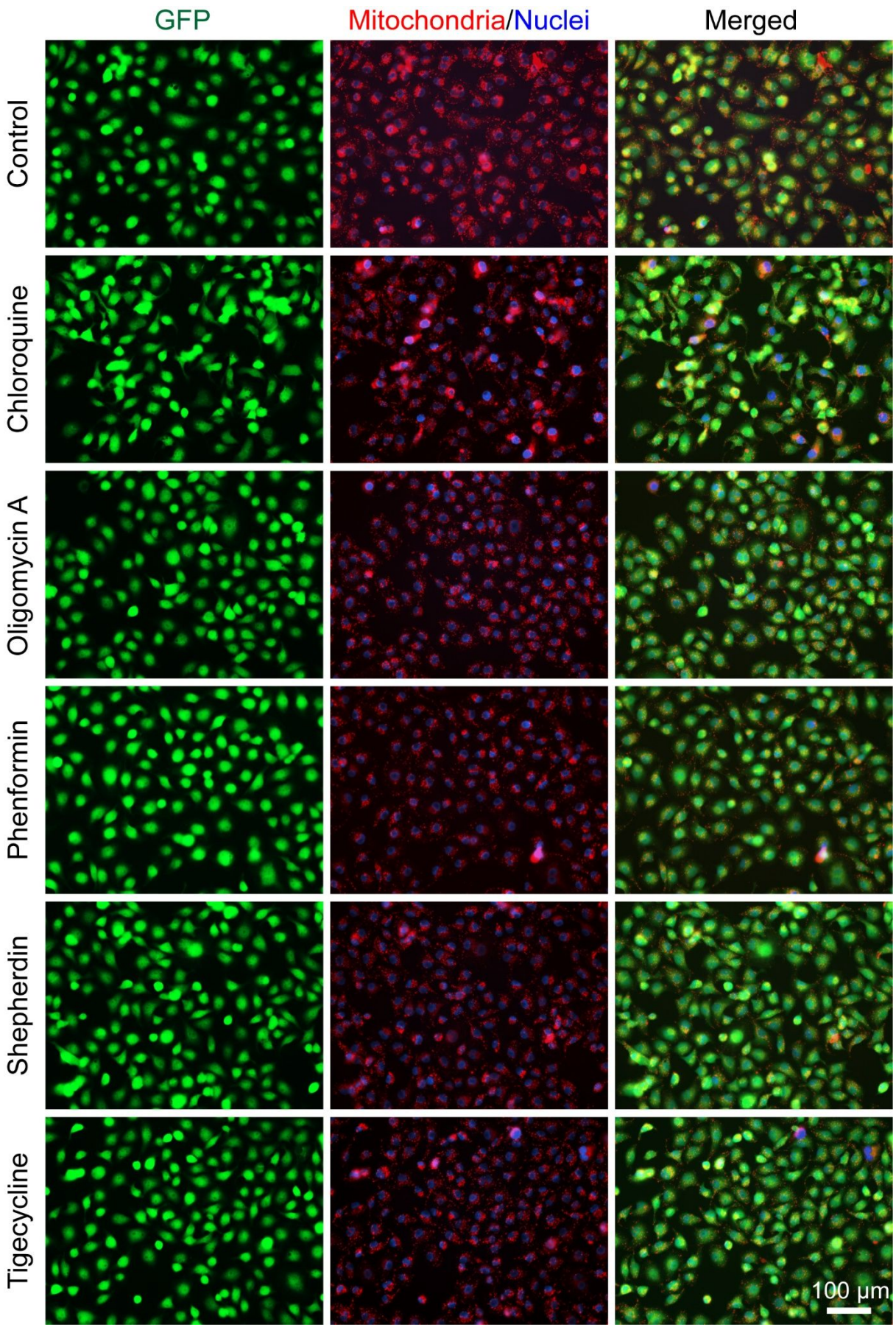
GFP
Mitochondria/Nuclei
Merged
Control
Chloroquine
Oligomycin A
Phenformin
Shepherdin
Tigecycline
100 μm

Figure S7. Morphology of MDA-MB-231/GFP cells treated with mitochondrial inhibitors and cultured in dishes for 6 h. Drugs were mixed with culture medium. Cells showed no observable differences with respect to different treatments, including non-treatment (control). Mitochondria and nuclei were labeled with MitoTracker Red and Hoechst 33342, respectively.

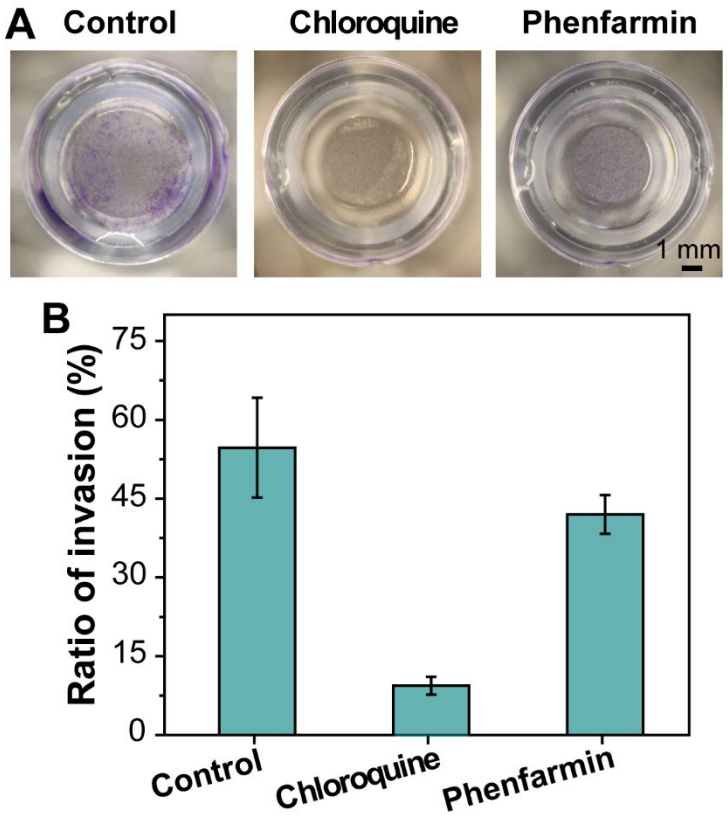

Figure S8. Invasion assay of MDA-MB-231 cells under the treatment of mitochondria-targeting drugs. (A) Representative images and (B) quantitative data showing much less cells (stained with crystal violet) invaded under the treatment of chloroquine (100 μM) compared to the control and phenfarmin (100 μM) treatment.

Table S1: List of GSEA clustered terms of protrusion samples.

Movie S1-S4

Movie S1: Dynamics of mitochondria trafficking during MDA-MB-231/GFP cells extending protrusions.

Movie S2: Untreated MDA-MB-231/GFP cells generated long cell protrusions within the PG-Chips.

Movie S3: MDA-MB-231/GFP cells treated with mdivi-1 (50 μM) generated short cell protrusions within the PG-Chips.

Movie S4: MDA-MB-231/GFP cells treated with chloroquine (100 μM) generated short cell protrusions within the PG-Chips.